



Building a database for brain 18 kDa translocator protein imaged using [¹¹C]PBR28 in healthy subjects

Soumen Paul¹, Evan Gallagher¹, Jehi-San Liow¹, Sanche Mabins¹, Katharine Henry¹, Sami S Zoghbi¹, Roger N Gunn², William C Kreisl³, Erica M Richards¹, Paolo Zanotti-Fregonara⁴, Cheryl L Morse¹, Jinsoo Hong¹, Aneta Kowalski¹, Victor W Pike¹, Robert B Innis¹ and Masahiro Fujita¹

Abstract

Translocator protein 18 kDa (TSPO) has been widely imaged as a marker of neuroinflammation using several radioligands, including [¹¹C]PBR28. In order to study the effects of age, sex, and obesity on TSPO binding and to determine whether this binding can be accurately assessed using fewer radio high-performance liquid chromatography (radio-HPLC) measurements of arterial blood samples, we created a database of 48 healthy subjects who had undergone [¹¹C]PBR28 scans (23 high-affinity binders (HABs) and 25 mixed-affinity binders (MABs), 20 F/28 M, age: 40.6 ± 16.8 years). After analysis by Logan plot using 23 metabolite-corrected arterial samples, total distribution volume (V_T) was found to be 1.2-fold higher in HABs across all brain regions. Additionally, the polymorphism plot estimated nondisplaceable uptake (V_{ND}) as 1.40 mL · cm⁻³, which generated a specific-to-nondisplaceable ratio (BP_{ND}) of 1.6 ± 0.6 in HABs and 1.1 ± 0.6 in MABs. V_T increased significantly with age in nearly all regions and was well estimated with radio-HPLC measurements from six arterial samples. However, V_T did not correlate with body mass index and was not affected by sex. These results underscore which patient characteristics should be accounted for during [¹¹C]PBR28 studies and suggest ways to perform such studies more easily and with fewer blood samples.

Keywords

Translocator protein, [¹¹C]PBR28, high-affinity binder, mixed-affinity binder, distribution volume

Received 1 August 2017; Accepted 12 February 2018

Introduction

Chronic—as opposed to acute—inflammation (also known as low grade inflammation) refers to a long-lasting subclinical inflammatory response¹ and has been associated with disorders such as diabetes,² coronary heart disease,³ and stroke,⁴ among others. Such inflammation is generally detected via blood tests for biomarkers like C-reactive protein (CRP), proinflammatory cytokines, tumor necrosis factor alpha (TNF- α), interleukin-6 (IL-6), and immune cells (T cells, macrophages, neutrophils, and eosinophils). Interestingly, advanced age,⁵ female sex,⁶ and obesity⁷ have all been linked to chronically elevated levels of these inflammatory markers in the periphery.

Positron emission tomography imaging of translocator protein (TSPO) 18 kDa⁸ provides a way to measure inflammation in the brain under pathological conditions associated with localized or more widespread

¹Molecular Imaging Branch, National Institute of Mental Health, National Institutes of Health, Bethesda, MD, USA

²Division of Brain Sciences, Department of Medicine, Imperial College London, London, UK; Imanova Centre for Imaging Sciences, London, UK

³Taub Institute, Columbia University Medical Center, New York, NY, USA

⁴Houston Methodist Research Institute, Houston, TX, USA

Corresponding author:

Masahiro Fujita, Molecular Imaging Branch, NIMH/NIH 10/B1D43, MSC 1026, 10 Center Drive, Bethesda, MD 20892, USA.

Email: masahiro.fujita@nih.gov

inflammatory changes.⁹ While TSPO levels are low in the CNS under physiological conditions, it is highly expressed in activated microglia and reactive astrocytes in the events of brain injury and inflammation, both of which are involved with the inflammatory response in the brain. However, it remains unknown whether age, sex, and obesity—which predispose to inflammation in the periphery—also do so in brain, which would identify these factors as important covariates in imaging studies of patients with neuropathology. The greatest barrier to assessing such predisposing factors in otherwise healthy subjects has been the small sample sizes of existing studies. For example, a previous study from our laboratory found no association between age and TSPO binding in brain, but the sample size was small ($n = 11$) and had a limited age range.¹⁰

To assess the association between neuroinflammation and age, sex, and obesity using TSPO as a putative biomarker, this study aggregated data from a large sample of healthy volunteers who had undergone [¹¹C]PBR28 imaging of TSPO. Towards this end, it is important to note that in the absence of reference tissue, quantitation of targets in brain typically requires arterial sampling in order to measure brain uptake and normalize for the amount of radioligand delivered to the brain in each subject. However, the number of arterial samples needed to accurately measure distribution volume (V_T) in brain using [¹¹C]PBR28 has not been determined. Thus, a secondary goal of this study was to investigate whether V_T can be accurately measured using a reduced number of arterial samples.

Methods

Radioligand synthesis

[¹¹C]PBR28 was synthesized as previously described,¹¹ with high radiochemical purity (>99%). Specific activity at the time of injection was 142 ± 80 GBq/ μ mol, the average injected activity was 672 ± 1.4 MBq, and the mass dose associated with these injections was 0.085 ± 0.063 nmol/kg.

Subjects

A total of 48 healthy subjects (23 high-affinity binders (HABs), 25 mixed-affinity binders (MABs)) were scanned after [¹¹C]PBR28 injection. TSPO affinity type was determined by in vitro receptor binding to TSPO on leukocyte membranes as previously described.¹² No low-affinity binders were included.¹³ Subjects were determined to be free of somatic or psychiatric illness, as assessed by medical history, physical examination, electrocardiogram (ECG), urinalysis, and

blood laboratory tests. The study was approved by the Institutional Review Board of the National Institutes of Health and Radiation Safety Committee, and complied with the Helsinki Declaration of 1975 (and as revised in 1983). All subjects gave written informed consent.

PET data acquisition

All healthy subjects underwent [¹¹C]PBR28 PET scans using an Advance PET scanner (GE Healthcare, GE Medical Systems, Waukesha, WI) with concurrent arterial blood sampling. A transmission scan was acquired prior to injection for attenuation correction. After [¹¹C]PBR28 injection, a dynamic emission scan was acquired for 90 min. Images were reconstructed using filtered backprojection with scatter and attenuation correction and a final resolution of full-width-at-half-maximum of approximately 7 mm.

Measurement of [¹¹C]PBR28 in blood samples

A total of 23 blood samples (varying from 1.0 to 5.0 mL each) were drawn throughout the 90-min scan period; these initially occurred in rapid succession (every 15 s) followed by longer intervals (every 15 min) towards the end. The selected time points for the 23 samples were 0.25, 0.5, 0.75, 1, 1.25, 1.5, 1.75, 2, 2.2, 2.5, 3, 4, 6, 8, 10, 15, 20, 30, 40, 50, 60, 75, and 90 min. For about 18 of the 23 samples, plasma [¹¹C]PBR28 concentrations were measured using high-performance liquid chromatography by separating radiometabolites (radio-HPLC).¹⁴ Radio-HPLC analysis was omitted for some of the early time points, where the fraction of [¹¹C]PBR28 in total plasma was greater than 0.9. For these time points, fraction of parent was linearly interpolated. The time activity curves of plasma [¹¹C]PBR28 concentrations were fitted to a tri-exponential function.

Image analysis

For each subject, a frame-based motion correction was applied to the dynamic PET image. Co-registration to the individual's MRI was subsequently accomplished using statistical parametric mapping (SPM 8; Wellcome Department of Cognitive Neurology, London, UK). A set of 78 predefined regions from the Hammers Probability Atlas was adjusted to the MRI scan of individual subjects using PNEURO/PMOD.¹⁵ These were segmented from the spatially normalized individual MRI and applied to the dynamic PET images. Total V_T was calculated by unconstrained two-compartment model, Logan plot,¹⁶ and Ichise MA1 multilinear analysis.¹⁷ In order to take into

account radioactivity in blood vessels, whole blood activity was used in the two-compartment model after linearly interpolating the activity between sampling times. For all brain areas, the volume of blood vessels was assumed to be 5% of the brain volume. In addition to the main analysis based on the regional data, V_T values were calculated in each voxel using Logan plot in order to visualize the overall distribution of TSPO binding. The parametric images of individual subjects were spatially normalized using SPM, and two average parametric images were then generated, one from all HABs and another from all MABs. The analyses were performed with PMOD 3.6 (PMOD Technologies, Zurich, Switzerland).

Effect of number of time points for arterial sampling

Conducting radio-HPLC analyses to determine the percentage of total radioactivity in plasma that represents parent radioligand is a time-consuming process. To assess the effect of number of blood samples analyzed with radio-HPLC on quantitation of V_T , three subsets of blood samples (6, 11, and 17) were randomly selected from the 23 original samples. Bias and variance of V_T from these three subsets were compared with the results generated from the full set of 23 timepoints. For each subset, different timepoints were used. The first subset used six timepoints (2, 6, 15, 30, 60, and 90 min); the second subset used 11 timepoints (0.5, 1, 2, 4, 10, 15, 20, 30, 50, 75, and 90 min); and the third subset used 17 timepoints (0.5, 1, 1.5, 2, 2.5, 4, 6, 8, 10, 15, 20, 30, 40, 50, 60, 75, and 90 min). The time activity curves of plasma [^{11}C]PBR28 concentrations from the six, 11, and 17 sample subsets were then fitted to a bi-exponential (but not a tri-exponential) function because of the reduced number of data points. V_{TS} calculated from the 6, 11, and 17 sample subsets were compared with V_T calculated from all 23 samples after fitting plasma [^{11}C]PBR28 concentrations to a tri-exponential function for the 23 samples.

Polymorphism plot to determine non-displaceable distribution volume

A polymorphism plot was used to estimate non-displaceable distribution volume (V_{ND}).¹⁸ In each of the predefined 78 brain areas of the Hammers Atlas, the V_{TS} of the right and left sides were averaged, with the exception of the corpus callosum and the brain stem (which have only one volume of interest (VOI)). Thus, 41 regions were used in the statistical analyses. For each of these regions, the mean V_T of MABs was subtracted from the mean V_T of HABs, and the difference was plotted against the mean V_T of HABs.

A linear regression was performed, and the x -intercept of the fitted line estimated V_{ND} . From this V_{ND} , and from the V_{TS} of HABs and MABs, a specific-to-non-displaceable ratio (BP_{ND}) between HABs and MABs could be calculated. The expected ratio of BP_{ND} between HABs and MABs is two, because MABs exhibit both high- and low-affinity phenotypes of TSPO, and the low-affinity phenotype does not have specific binding of [^{11}C]PBR28 detectable with PET.¹⁹ However, when testing whether the BP_{ND} ratio is close to two, it is important to take into account the statistical uncertainty of the polymorphism plot, i.e. linear regression. To account for this uncertainty, we tested whether the slope of the polymorphism plot was significantly different from 0.5. A BP_{ND} ratio for HABs/MABs = 2 is the same as a slope = 0.5 because the slope is defined as the V_T values of (HABs – MABs)/HABs.

Partial volume correction

We assessed the effects of age, BMI, and sex using PET data with and without partial volume correction (PVC) because aging in adulthood is associated with decreased gray matter volume.²⁰ A geometric transfer matrix method²¹ was applied to correct spill-in and spill-out between brain areas.

Statistical analysis

The association between V_T and age or BMI was examined by partial correlation, where TSPO genotype was used as a covariate. BMI was determined as the subject's weight in kilograms divided by the square of their height in meters ($\text{kg} \cdot \text{m}^{-2}$). As a secondary analysis, a multiple regression was performed for whole brain where V_T was used as the dependent variable, and sex, age, and BMI were used as independent variables. In this analysis, V_{TS} of MABs were multiplied by 1.2 to make them equivalent to those of HABs. Gender differences in V_T were examined using a univariate analysis of variance with age as a covariate. Age was included as a covariate because of the significant correlation between V_T and age (Figure 3(c)). Linear regression analyses were applied to compare V_T by 23 samples (as well as within the three smaller subsets of samples) and for the polymorphism plot.

The partial correlation analyses and univariate analysis of variance were performed in IBM SPSS Statistics (version 23 for windows; SPSS INC., Chicago, IL, USA). Linear regression analyses were performed in Prism 5 (GraphPad software, Inc., La Jolla, CA, USA). The deviation of the slope of the polymorphism plot from 0.5 was tested by t -test.

Results

Demographic data

Of the 48 subjects in this analysis, 23 were HABs (13 M, 10 F) and 25 were MABs (15 M, 10 F) (Table 1).

Plasma parent and brain time activity curves

After [¹¹C]PBR28 injection, the tracer readily entered the brain and showed widespread distribution. Peak brain uptake for HABs and MABs was around 1.9 and 1.8 SUV, respectively, followed by moderate washout (Figure 1(a)). Peak parent plasma concentrations for both HABs and MABs were similar, with slightly faster washout in MABs (Figure 1(b)). The parent fraction was estimated to be 18% of the total radioactivity in plasma at 30 min after radioligand injection and was reduced to 5% at 90 min (Figure 1(c)).

Kinetic analysis

Using PET data without PVC, we compared three methods to quantify V_T : an unconstrained two compartment model, Logan plot, and Ichise multilinear analysis (MA1). Of these, the Logan plot was selected for subsequent analyses because: (1) it did not give non-physiologic V_T s (that is, markedly high or negative values) in any region; and (2) it underestimated V_T by only 5.5% relative to the two-compartment model. In contrast, the two-compartment model did not identify V_T well in 10% of datasets, with standard errors noted at greater than 10%. In these datasets, V_T s became unphysiologically large; for example, a small subset of brain regions yielded V_T values greater than $100 \text{ mL} \cdot \text{cm}^{-3}$ due to poorly identified small k_4 values. The Ichise MA1 yielded similar, but slightly poorer, results than the Logan plot; specifically, it underestimated V_T relative to the two-compartment model by 7.5% and gave non-physiologic V_T values in four regions. The V_T of whole brain from Logan plot was 19% higher in HABs than in MABs (3.7 ± 0.9 vs. 3.0 ± 0.9 , respectively).

Table 1. Subject demographics.

	HABs (n = 23)	MABs (n = 25)
Age (y)	40.3 ± 15.5	41.0 ± 18.2
Age range (y)	21–71	21–70
Race	10C, 8AA, 4A, 1L	19C, 5AA, 1L
Sex	13 M, 10 F	15 M, 10 F

HAB: high-affinity binder; MAB: mixed-affinity binder; C: Caucasian; AA: African-American; L: Latino; A: Asian.

Parametric V_T images

Logan parametric images of V_T showed widespread distribution of [¹¹C]PBR28 binding consistent with the results obtained using regional data. No region showed markedly low V_T , which could indicate little presence of specific binding (Figure 2).

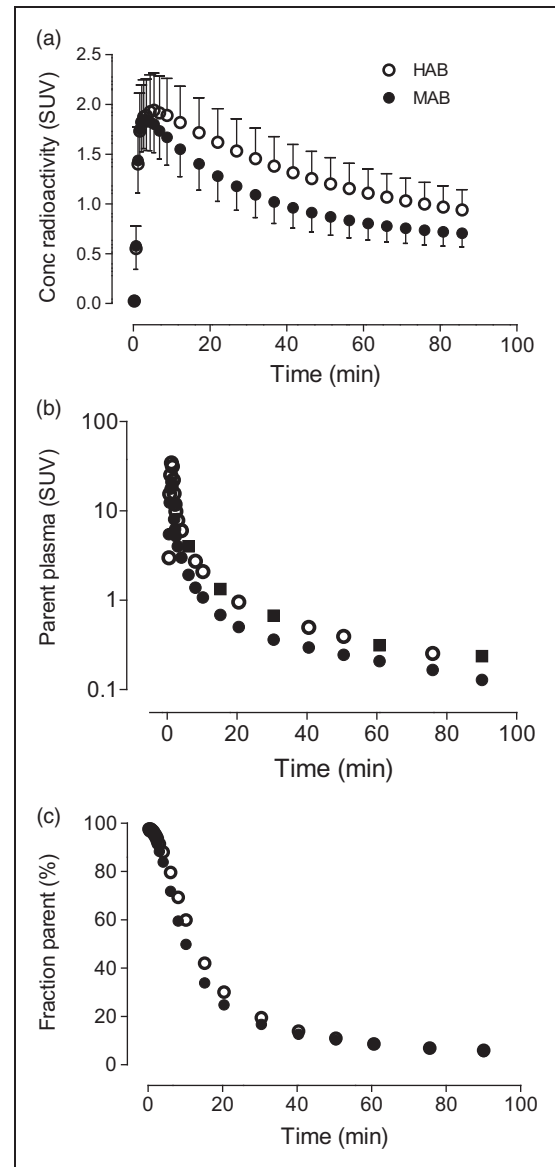


Figure 1. (a) Mean concentrations of radioactivity in whole brain for high-affinity binders (HABs) and mixed-affinity binders (MABs) as a function of time. (b) [¹¹C]PBR28 concentrations in arterial plasma as a function of time. The timepoints shown with closed squares represent the six samples used to assess whether a smaller number of plasma samples can accurately measure distribution volume (V_T). (c) The percentage of total radioactivity in plasma that represents parent radioligand separated from radiometabolites.

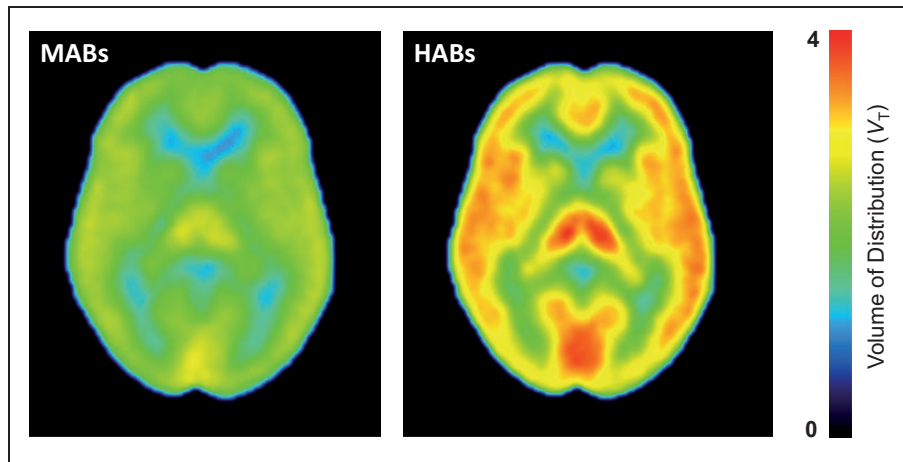


Figure 2. Mean Logan parametric PET images of high-affinity binders (HABs) and mixed-affinity binders (MABs). Each pixel value represents V_T and is indicated in V_T color scale.

Influence of sex, age, and BMI on [^{11}C]PBR28 binding in brain

To the best of our knowledge, previous PET studies have not reported a significant influence of age, BMI, or gender on TSPO levels in specific brain areas, we first performed statistical analyses in each of the 41 VOIs to explore whether these three parameters influenced certain VOIs more than others. Because influence of any of these variables did not markedly differ among the VOIs, a whole brain region (i.e., a volume weighted average of all VOIs) was used for the primary results. Across all regions, V_T did not differ between males and females (Figure 3(a)), nor did it correlate with BMI (Figure 3(b)), with or without PVC.

In contrast, V_T was significantly and positively correlated with age in nearly all regions, both with and without PVC. Without PVC, the correlation between V_T and age was significant in 37 of the 41 brain regions ($r^2=0.088\text{--}0.2116$, $P=0.01\text{--}0.042$, Figure 3(c)). The four regions without a significant correlation were the subcallosal area, the postcentral gyrus, the superior parietal gyrus, and the caudate nucleus. The substantia nigra and pallidum were excluded from the correlation because PVC markedly increased noise in these two small regions. With the exclusion of these two regions, correlation was significant in 35 of the remaining 39 regions ($r^2=0.13\pm 0.06$ and $P=0.019\pm 0.03$ without PVC, and $r^2=0.16\pm 0.07$ and $P=0.015\pm 0.03$ with PVC, respectively).

Because of the significant correlation between V_T and age in most regions except the small ones, we assessed the overall magnitude of the effect via a whole brain VOI. This correlation was significant both with ($r^2=0.20$ and $P=0.001$) and without

($r^2=0.11$ and $P=0.021$) PVC. The slopes (ΔV_T per annum) of these linear correlations were 0.033 with PVC and 0.018 without PVC. In other words, V_T increased by 7.3% (with PVC) or 4.7% (without PVC) per decade of life (e.g. from age 50 to age 60). These slopes were calculated from the combined data of HABs and MABs after scaling the V_T of MABs by 1.3 and 1.2 for V_T with and without PVC, respectively. BP_{ND} , which reflects only specific binding, increased by 11.3% (with PVC) or 7.8% (without PVC) from age 50 to 60 by assuming no age-related changes in V_{ND} .

A multiple regression using sex, age, and BMI as independent variables confirmed that age was the only variable among the three to significantly influence V_T ($P=0.024$). The influences of BMI ($P=0.104$) and sex ($P=0.325$) were not significant.

Effect of reduced number of arterial samples on V_T

To investigate the accuracy of measuring V_T via a smaller number of arterial blood samples, we compared V_T determined with the complete set of 23 samples to V_T s determined with 6, 11, and 17 samples. Because samples around the peak plasma levels were not included, the reduced-sample subsets misidentified V_T in all cases, as indicated by slopes different than 1 in the correlations (Table 2). The overestimation was 10% for six samples, and the underestimation was 2% for both 11 and 17 samples. Nevertheless, V_T obtained by these three subsets correlated well ($r^2\geq 0.91$) with that calculated using all 23 samples (Table 2, Figure 4). In other words, while the subsets had biases ranging from 2% to 10%, their overall precision relative to all 23 samples was quite good ($r^2\geq 0.91$).

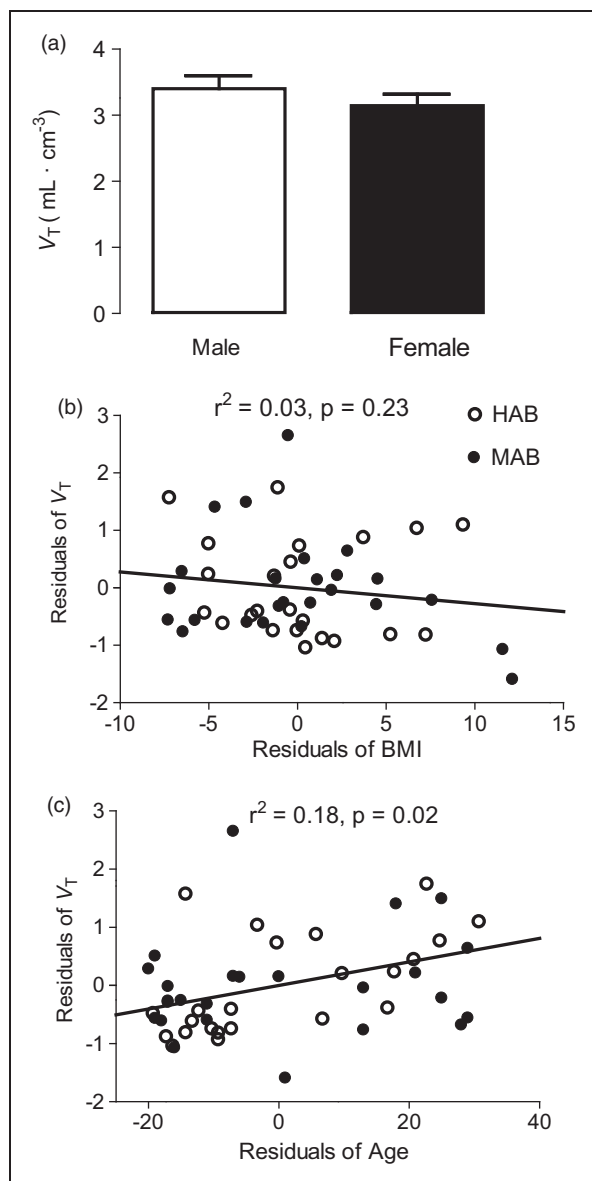


Figure 3. Effect of (a) sex, (b) body mass index (BMI), and (c) age on distribution volume (V_T) of [¹¹C]PBR28. For clarity of presentation, panel A shows the high-affinity binder equivalent values of V_T for whole brain, calculated by multiplying the V_T of mixed-affinity binders (MABs) by 1.2. Panels B and C show unstandardized residuals used in the partial correlations where genotype was used as a covariate.

Polymorphism plot

V_{ND} estimated by the x -intercept of the polymorphism plot was 1.4 mL · cm⁻³ (95% CI 0.6–1.8) (Figure 5) based on results from 41 brain regions. Using this value, BP_{ND} (mL · cm⁻³) in whole brain was found to be 31% higher in HABs (1.6 ± 0.6) than in MABs (1.1 ± 0.6). The BP_{ND} ratio—which is equivalent to the ratio of specific binding—was 1.4 for HABs/MABs.

Table 2. Measuring V_T with a decreasing number of plasma samples.

Samples	$V_T \pm SD$	Slope	r^2
23	3.7 ± 0.9	1.00	1.00
17	3.7 ± 0.9	0.98	0.94
11	3.7 ± 1.0	0.98	0.94
6	4.0 ± 1.1	1.10	0.91

Note: Deviation of the slope from 1.0 provided accuracy relative to all 23 samples. For example, a slope of 1.10 for the six-sample subset implies that this smaller number of samples overestimated V_T by 10%. The correlation coefficient (r^2) measures how well the smaller number of samples substitutes for the V_T calculated using the entire 23 timepoints.

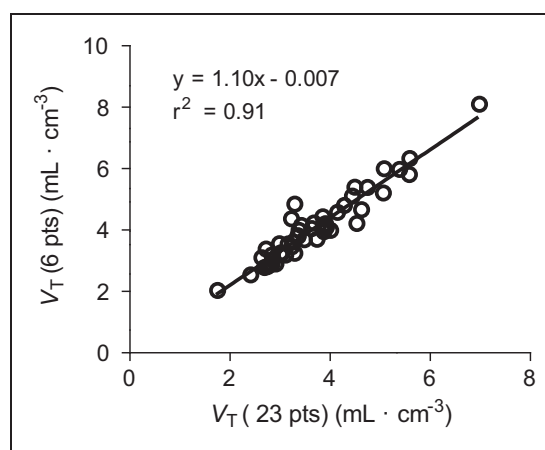


Figure 4. Correlation of whole brain distribution volume (V_T) calculated from 23 plasma measurements with that calculated from six timepoints. The slope (1.10) implies that using six timepoints overestimated V_T by 10% compared to V_T from all 23 time points.

The slope of the linear regression was 0.33, which was significantly smaller than 0.5 ($P = 0.0003$). This significant deviation from 0.5 means that the BP_{ND} ratio of HABs/MABs was significantly smaller than two.

Discussion

This study measured the effects of age, sex, and BMI on TSPO binding in brain using a database of 48 healthy subjects. We found that total brain uptake (V_T) of [¹¹C]PBR28 positively correlated with age ($P = 0.019$; $r^2 = 0.18$) but did not correlate with BMI or differ between the sexes. We also assessed the accuracy of measuring V_T using a smaller number of arterial samples than the full set of 23. We found that V_T calculated from six plasma samples, each of which measured the concentration of parent radioligand separated from radiometabolites, was highly correlated ($r^2 = 0.91$)

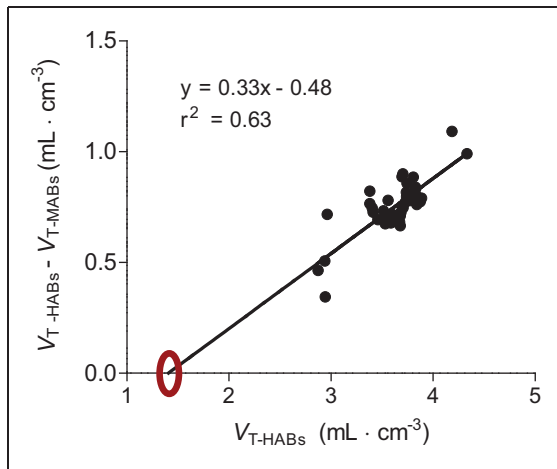


Figure 5. Polymorphism plot to estimate nondisplaceable uptake (V_{ND}) in an imaginary region with no specific binding (x -intercept). For 41 different brain regions, the distribution volume (V_T) in mixed-affinity binders (MABs) was subtracted from that in high-affinity binders (HABs) and plotted against the distribution volume (V_T) of HABs. The extrapolated x -intercept marked with a circle shows that the estimated V_{ND} for this population was $1.4 \text{ mL} \cdot \text{cm}^{-3}$.

with that from the entire set and only overestimated V_T by 10%.

Prior studies

Our findings indicate that TSPO expression in brain increases with age, a result consistent with findings from a postmortem study of neurologically normal individuals (ages two to 80) that found age-related increases in microglial expression in all brain regions.²² Although the current study used the largest sample size thus far ($n = 48$), prior PET studies have been markedly inconsistent, which makes it difficult to draw firm conclusions regarding the relationship between age and in vivo TSPO expression. While some studies^{23–25} reported widespread increases in TSPO expression in most brain regions, others^{26–28} found no change, and one even reported an age-related increase in TSPO expression only in the thalamus and not in any other regions.²⁹

Several explanations may account for the inconsistencies mentioned above, including study-to-study differences in the way TSPO binding was measured, differences in the PET ligand used, and demographic differences between study populations. However, it should be noted that ours and one of the seven studies²⁶ reported V_T , which is an absolute measure of binding that normalizes brain uptake to a metabolite-corrected arterial input function; the remaining studies investigating this issue had no such absolute measure (Supplementary Table 1). Interestingly, while our study

included more subjects than Suridjan et al., that study found no age-related increases in TSPO expression despite having the second largest sample size ($n = 33$). This discrepancy could potentially be investigated by merging the two datasets and subsequently re-analyzing the expanded database ($n = 81$). Such a database might also allow us to investigate other unknown parameters that influence TSPO levels. Unfortunately, any such analysis would be complicated by the fact that each PET ligand has a different affinity ratio of HABs to MABs, and this makes combining data from multiple studies challenging. One solution could be to generate V_{ND} values using the polymorphism plot, calculate ratios of BP_{ND} between HABs and MABs for each ligand, scale BP_{ND} s of MABs to those of HABs, and then combine the resulting data. However, this method might introduce a substantial source of error due to the uncertainty associated with calculating BP_{ND} via the polymorphism plot. In the current study, for example, the 95% CI for BP_{ND} was 0.6–1.8. If this additional uncertainty is undesirable, a simpler way to combine datasets would be to only include studies that used the same PET ligand.

We note that the present study, by itself, cannot determine whether aging is associated with neuroinflammation. Instead, these results merely underscore the correlation between TSPO binding and age in healthy subjects. In this context, it should be noted that while TSPO is a *putative* biomarker of neuroinflammation, its use for this purpose will require more study in both healthy subjects and in patients suffering from a variety of inflammation-associated disorders.

The present study found no correlation between V_T and BMI, consistent with at least one prior study that investigated the correlation between [¹¹C]PBR28 binding and BMI in healthy as well as depressed subjects.³⁰ As noted previously, obesity has been linked to increased production of proinflammatory cytokines such as TNF- α and IL-6.⁷ However, the present study found no correlation between TSPO binding and BMI even after controlling for genotype.

With regard to the links between TSPO expression and inflammation in general, several studies of TSPO binding in neurological disorders found either localized or relatively global upregulation,^{31,32} providing strong evidence that TSPO may be a useful biomarker of neuroinflammation. However, in other disorders—for instance, multiple sclerosis—no clear relationship between disease status and TSPO uptake has been observed,²⁶ suggesting that the usefulness of TSPO imaging may vary depending on the type and progression of the disorder in question. Furthermore, the largely positive findings in several neurological disorders do not necessarily mean that TSPO density is a marker of neuroinflammation in healthy subjects. In fact,

TSPO binding in healthy subjects in this study was associated with a fairly large COV (24% in this population after correcting for genotype), suggesting considerable variability.

Effect of genotype

Previous studies found that the average V_T of HABs was less than twice that of MABs, a result explained by the fact that V_T includes both specific¹³ and nondisplaceable (V_{ND}) uptake.⁸ While V_S of HABs might be twice that of MABs, V_{ND} would be expected to be the same in both groups, thereby making the V_T of HABs less than twice that of MABs. In contrast, BP_{ND} is a measure of specific binding (normalized to V_{ND}). In the present study, the value of BP_{ND} in HABs was also less than twice that in MABs. Specifically, the ratio of BP_{ND} in HABs (1.6) was only 1.4 times larger than the ratio in MABs (1.1). Based on in vitro studies, we had expected the BP_{ND} of HABs to be twice that of MABs, i.e. the slope of Figure 4 would be 0.5. The cause of this significant deviation from a BP_{ND} ratio of two is not clear, but a possible cause is that the polymorphism plot was performed using data from different subjects rather than from the same subjects scanned under two different conditions, i.e. baseline and blocked scans. In fact, another study from our laboratory using a different TSPO ligand, [¹¹C]DPA-713, similarly obtained different BP_{ND} ratios from polymorphism and occupancy plots.³³ It should be noted that a separate [¹¹C]PBR28 study reported similar BP_{ND} ratios of HABs and MABs as determined by polymorphism and occupancy plots, but the sample size in that study was much smaller.³⁴ Another possible cause for the lower BP_{ND} ratio is that radioligand binding could differ between in vitro and in vivo conditions, as previously reported for another TSPO ligand, [¹¹C]ER176.³⁵

Accurate measurement of TSPO density in brain

As a secondary goal of the study, we used this dataset to assess how many plasma samples were needed to accurately measure the density (i.e. V_T) of TSPO in brain. To do this, we assumed that the complete set of 23 samples was correct and compared the results obtained via this larger number of samples to analyses conducted with 6, 11, and 17 sample subsets. We found that the V_T values obtained from six samples significantly correlated with the V_T value calculated from 23 samples ($r^2=0.91$), with an overestimation of 10%. This overestimation was caused by a failure to capture the peak of the plasma time-activity curve; thus, underestimating the input function overestimated V_T .

Assuming that this overestimation applies equally to patients and healthy volunteers, six samples for radiometabolite analysis seem fully adequate for research studies, a finding that has significant implications for improving V_T quantitation. However, the accuracy of measurements using six samples may need to be validated by comparing healthy subjects and patients, particularly if inflammation in peripheral organs such as lung occurs in the patient group, given that peripheral inflammation might affect the shape of the input function.

Larger goal: Sharing via a database

Although the specific aim of this study was to determine whether age, sex, or BMI affected TSPO density in brain, it also had the broader goal of creating a public database that could be used to share primary data (including PET, MRI, and plasma measurements) for the purposes of data mining or as a way to compare patient results. While working towards this larger goal, two key barriers emerged. First, the gradual shift over time in our own methods of image reconstruction and data analysis, and second, significant regulatory barriers to sharing primary data.

With regard to the first issue, this group of healthy subjects was drawn from several protocols conducted over a decade. The initial protocol had merely sought to evaluate [¹¹C]PBR28, while subsequent studies recruited new subjects as controls for various patient populations, including Alzheimer's disease, autism, depression, and epilepsy. In addition to the difficulties associated with retrieving study-related information from several investigators who had left our laboratory, we found that some acquisition or reconstruction parameters had changed over the past 10 years.^{36,37} To address this issue, we restricted the analysis to scans performed using one camera (GE Advance), reconstructed data as necessary, and uniformly analyzed the images. Nevertheless, we had to exclude several subjects because of missing variables (e.g. no genotype results were available for subjects who had participated in these studies before the HAB/MAB/LAB genotype was discovered) or because of lack of uniformity (e.g. incomplete plasma data from subjects who had not provided 23 plasma samples). Thus, some data were lost even within our own internal analyses.

With regard to the second issue, we discovered that we were not permitted to share the primary results (e.g. PET, MRI, and plasma measurements) even when completely anonymized. Although such sharing would have been possible in past years, new regulations at the NIH and many other institutions allow sharing of primary data only if such sharing is specifically described in the

consent form. Unfortunately, that language did not appear in the consent forms of these subjects, who had been scanned over a 10-year period. To overcome this barrier, we would have needed to re-consent the subjects, a cumbersome process at best and one that is often impossible for subjects who have moved away and left no means of contacting them. To avoid such difficulties in the future, we recommend that investigators establish standard formats for data collection and ensure that consent forms allow the results to be shared after appropriate anonymization. These recommendations could be helpful not only for data sharing, but also for achieving uniformity of data within a single laboratory.

Conclusion

In this study, we found that TSPO expression measured in healthy subjects using [¹¹C]PBR28 correlated positively with age, but not with BMI, and was not affected by sex. This suggests that future TSPO imaging studies should either control for age during recruitment or correct for age post-hoc. We also found that six plasma samples with radio-HPLC measurements were capable of adequately measuring the concentration of parent radioligand in arterial plasma, though we further recommend that such samples be supplemented with additional sample measures of total radioactivity in either whole blood or plasma.

Funding

The author(s) disclosed receipt of the following financial support for the research, authorship, and/or publication of this article: This study was funded by the Intramural Research Program of the National Institute of Mental Health, NIH: projects ZIAMH002852 and ZIAMH002793 under clinical protocols NCT01547780, NCT00526916, NCT01322555, NCT01851356, NCT02233868 and NCT00613119.

Acknowledgements

We gratefully acknowledge the dedicated staff of the Molecular Imaging Branch of the NIMH and the PET Department of NIH's Clinical Center for help in successfully completing these studies. Ioline Henter (NIMH) provided excellent editorial assistance, Sun Jung Kang, Yin Yao and Wei Guo (Statistical Genomics and Data Analysis Core, Intramural Research programs, NIH) for the assistance with the statistical analysis.

Declaration of conflicting interests

The author(s) declared the following potential conflicts of interest with respect to the research, authorship, and/or publication of this article: Dr. Gunn is an employee of Imanova Ltd. The remaining authors have no conflict of interest to disclose, financial or otherwise.

Authors' contributions

Soumen Paul, Evan Gallagher, Jieih-San Liow, Sami S Zoghbi, Cheryl L Morse, Jinsoo Hong, substantially contributed to acquisition, analysis, and interpretation of data; drafted article and revised it critically for important intellectual content.

Sanche Mabins, Katharine Henry, Roger N Gunn, William C Kreisl, Erica M Richards, Paolo Zanotti-Fregonara, Aneta Kowalski, Victor W Pike, Robert B Innis, substantially contributed to the conception and design of the study; drafted the article and revised it critically for important intellectual content.

Masahiro Fujita substantially contributed to the conception and design of the study; contributed substantially to the acquisition, analysis, and interpretation of data; drafted the article and revised it critically for important intellectual content.

Supplementary material

Supplementary material for this paper can be found at the journal website: <http://journals.sagepub.com/home/jcb>

References

- Hotamisligil GS. Inflammation and metabolic disorders. *Nature* 2006; 444: 860–867.
- Wellen KE and Hotamisligil GS. Inflammation, stress, and diabetes. *J Clin Invest* 2005; 115: 1111–1119.
- Danesh J, Whincup P, Walker M, et al. Low grade inflammation and coronary heart disease: prospective study and updated meta-analyses. *BMJ* 2000; 321: 199–204.
- Ishikawa J, Tamura Y, Hoshida S, et al. Low-grade inflammation is a risk factor for clinical stroke events in addition to silent cerebral infarcts in Japanese older hypertensives: the Jichi Medical School ABPM Study, wave 1. *Stroke* 2007; 38: 911–917.
- Lencel P and Magne D. Inflammaging: the driving force in osteoporosis? *Med Hypotheses* 2011; 76: 317–321.
- McConnell JP, Branum EL, Ballman KV, et al. Gender differences in C-reactive protein concentrations-confirmation with two sensitive methods. *Clin Chem Lab Med* 2002; 40: 56–59.
- Miller AA and Spencer SJ. Obesity and neuroinflammation: a pathway to cognitive impairment. *Brain Behav Immun* 2014; 42: 10–21.
- Kreisl WC, Jenko KJ, Hines CS, et al. A genetic polymorphism for translocator protein 18kDa affects both in vitro and in vivo radioligand binding in human brain to this putative biomarker of neuroinflammation. *J Cerebr Blood Flow Metab* 2013; 33: 53–58.
- Chen MK and Guilarte TR. Translocator protein 18 kDa (TSPO): molecular sensor of brain injury and repair. *Pharmacol Ther* 2008; 118: 1–17.
- Kreisl WC, Lyoo CH, Liow JS, et al. (11)C-PBR28 binding to translocator protein increases with progression of Alzheimer's disease. *Neurobiol Aging* 2016; 44: 53–61.

11. Briard E, Zoghbi SS, Imaizumi M, et al. Synthesis and evaluation in monkey of two sensitive ¹¹C-labeled aryloxyanilide ligands for imaging brain peripheral benzodiazepine receptors in vivo. *J Med Chem* 2008; 51: 17–30.
12. Kreisl WC, Jenko KJ, Hines CS, et al. A genetic polymorphism for translocator protein 18 kDa affects both in vitro and in vivo radioligand binding in human brain to this putative biomarker of neuroinflammation. *J Cereb Blood Flow Metab* 2013; 33: 53–58.
13. Hines CS, Fujita M, Zoghbi SS, et al. Propofol decreases in vivo binding of ¹¹C-PBR28 to translocator protein (18 kDa) in the human brain. *J Nucl Med* 2013; 54: 64–69.
14. Zoghbi SS, Shetty HU, Ichise M, et al. PET imaging of the dopamine transporter with ¹⁸F-FECNT: a polar radiometabolite confounds brain radioligand measurements. *J Nucl Med* 2006; 47: 520–527.
15. Hammers A, Allom R, Koeppe MJ, et al. Three-dimensional maximum probability atlas of the human brain, with particular reference to the temporal lobe. *Hum Brain Mapp* 2003; 19: 224–247.
16. Logan J, Fowler JS, Volkow ND, et al. Graphical analysis of reversible radioligand binding from time-activity measurements applied to [¹¹C-methyl]-(-)-cocaine PET studies in human subjects. *J Cereb Blood Flow Metab* 1990; 10: 740–747.
17. Ichise M, Toyama H, Innis RB, et al. Strategies to improve neuroreceptor parameter estimation by linear regression analysis. *J Cereb Blood Flow Metab* 2002; 22: 1271–1281.
18. Guo Q, Colasanti A, Owen DR, et al. Quantification of the specific translocator protein signal of ¹⁸F-PBR111 in healthy humans: a genetic polymorphism effect on in vivo binding. *J Nucl Med* 2013; 54: 1915–1923.
19. Owen DR, Gunn RN, Rabiner EA, et al. Mixed-affinity binding in humans with 18-kDa translocator protein ligands. *J Nucl Med* 2011; 52: 24–32.
20. Kalpouzos G, Chetelat G, Baron JC, et al. Voxel-based mapping of brain gray matter volume and glucose metabolism profiles in normal aging. *Neurobiol Aging* 2009; 30: 112–124.
21. Rousset O, Rahmim A, Alavi A, et al. Partial volume correction strategies in PET. *PET Clin* 2007; 2: 235–249.
22. Sheng JG, Mrak RE and Griffin WS. Enlarged and phagocytic, but not primed, interleukin-1 alpha-immunoreactive microglia increase with age in normal human brain. *Acta Neuropathologica* 1998; 95: 229–234.
23. Kumar A, Muzik O, Shandal V, et al. Evaluation of age-related changes in translocator protein (TSPO) in human brain using ¹¹C-[R]-PK11195 PET. *J Neuroinflammation* 2012; 9: 232.
24. Gulyás B, Vas A, Tóth M, et al. Age and disease related changes in the translocator protein (TSPO) system in the human brain: positron emission tomography measurements with [¹¹C]vinpocetine. *Neuroimage* 2011; 56: 1111–1121.
25. Schuitemaker A, van der Doef TF, Boellaard R, et al. Microglial activation in healthy aging. *Neurobiol Aging* 2012; 33: 1067–1072.
26. Suridjan I, Rusjan PM, Voineskos AN, et al. Neuroinflammation in healthy aging: a PET study using a novel Translocator Protein 18kDa (TSPO) radioligand, [(18)F]-FEPPA. *Neuroimage* 2014; 84: 868–875.
27. Debruyne JC, Versijpt J, Van Laere KJ, et al. PET visualization of microglia in multiple sclerosis patients using [¹¹C]PK11195. *Eur J Neurol* 2003; 10: 257–264.
28. Yasuno F, Ota M, Kosaka J, et al. Increased binding of peripheral benzodiazepine receptor in Alzheimer's disease measured by positron emission tomography with [¹¹C]DAA1106. *Biol Psychiatry* 2008; 64: 835–841.
29. Cagnin A, Brooks DJ, Kennedy AM, et al. In-vivo measurement of activated microglia in dementia. *Lancet* 2001; 358: 461–467.
30. Hannestad J, DellaGioia N, Gallezot JD, et al. The neuroinflammation marker translocator protein is not elevated in individuals with mild-to-moderate depression: a [(1)(1)C]PBR28 PET study. *Brain Behav Immun* 2013; 33: 131–138.
31. Jacobs AH and Tavitian B. Noninvasive molecular imaging of neuroinflammation. *J Cereb Blood Flow Metab* 2012; 32: 1393–1415.
32. Vivash L and O'Brien TJ. Imaging microglial activation with TSPO PET: lighting up neurologic diseases? *J Nucl Med* 2016; 57: 165–168.
33. Kobayashi M, Jiang T, Telu S, et al. ¹¹C-DPA-713 has much greater specific binding to translocator protein 18 kDa (TSPO) in human brain than ¹¹C-(R)-PK11195. *J Cereb Blood Flow Metab* 2017; 38: 393–403.
34. Owen DR, Guo Q, Kalk NJ, et al. Determination of [(11)C]PBR28 binding potential in vivo: a first human TSPO blocking study. *J Cereb Blood Flow Metab* 2014; 34: 989–994.
35. Ikawa M, Lohith TG, Shrestha S, et al. ¹¹C-ER176, a radioligand for 18-kDa translocator protein, has adequate sensitivity to robustly image all three affinity genotypes in human brain. *J Nucl Med* 2017; 58: 320–325.
36. Hirvonen J, Kreisl WC, Fujita M, et al. Increased in vivo expression of an inflammatory marker in temporal lobe epilepsy. *J Nucl Med* 2012; 53: 234–240.
37. Kreisl WC, Lyoo CH, Liow J-S, et al. Distinct patterns of increased translocator protein in posterior cortical atrophy and amnesic Alzheimer's disease. *Neurobiol Aging* 2017; 51: 132–140.